Iranian Society of Acoustics and Vibration
The 14th ISAV2024 International Conference on Acoustics and Vibration
11-12 Dec 2024 Karaj - Iran
Kharazmi University

Nonlinear dynamics and stability assessment of a flexible rotor-disk-bearing system incorporating bearing flexibility

Mohammad Amin Ghasemi[a], Morteza Karamooz Mahdiabadi[a*], Saeed Bab[b]

[a] *Department of Mechanical Engineering, Tarbiat Modares University, P.O. Box 14115-177, Tehran, Iran*

[b] *Mechanical Rotary Equipment Department, Niroo Research Institute, Dadman street, P.O. Box 14665-517, Tehran, Iran*

* *Corresponding author: karamooz@modares.ac.ir*

Abstract

This study presents a nonlinear dynamic analysis of a rotor-disk-bearing system consisting of a flexible continuous rotor supported by two flexible bearings. The rotor incorporates rigid disks positioned equidistantly with zero phase difference. Both linear and nonlinear characteristics of the bearings are considered. The system's governing equations are derived using Hamilton's principle, treating the rotor as an Euler-Bernoulli beam to obtain partial differential equations. Mode shapes of a rotating beam on two springs are employed to discretize the equations via Galerkin's method, yielding ordinary differential equations. Multiple scales analysis is applied to solve the equations analytically and investigate the effects of various parameters such as linear and nonlinear bearing stiffness coefficients on stability. Frequency response curves are generated to analyze dynamic behavior. Numerical integration using the Runge-Kutta method validates the analytical solutions and excellent agreement is observed. The analyses provide insights on system behavior under flexible bearing support incorporating nonlinear dynamics.

Keywords: Rotating systems; multiple scales method ; flexible bearings; stationary analysis .

1. Introduction

Rotating systems are employed in various industries, including power plant turbines, automotive and manufacturing. These machines typically feature a moving part known as a turbine. With industrial advancements and increased rotational speeds of these machines, studying the dynamic and vibrational behavior of these systems has become increasingly important.

Rotating systems are modeled in various forms and have different characteristics. for instance, in different loading conditions, Fadatari et al. [1] investigated the effects of an axial load under different excitation frequencies and unbalanced mass eccentricity, while Moradi et al. [2] examined

the influence of gravitational forces on the system's dynamic behavior. Sadooghi et al. [3] studied a rotor-disk system with bearings under stationary conditions.

Bearings are a crucial component in dynamic analysis of rotating systems, and they come in various types. Jain et al. [4] conducted mathematical modeling of bearings in rotating systems, considering factors such as radial clearance and the number of balls. Liang et al. [5] examined the effect of roller bearing parameters on the nonlinear dynamics of offset rotors. in practice, bearings exhibit nonlinear stiffness and damping properties. to assess the impact of nonlinear stiffness and damping, as well as to compare linear and nonlinear stiffness and damping in frequency response and force transmission, Caiyer et al. [6] proposed a model for evaluating these coefficients.

Zhang et al. [7] derived the equations of motion for a system with third-order nonlinear stiffness and clearance using Lagrange's equations, employing harmonic balance and Runge-Kutta methods to solve the dynamic response. To examine the primary resonance of a shaft with simple supports and large vibration amplitudes, a shaft with distributed mass can be considered [8].

Guanzhou et al. [9] studied the characteristics of combination and primary resonance in a dual-rotor system under simultaneous impact with the bearing between the shafts. In this study, the simultaneous impact of the shaft with the third bearing, considering the nonlinear complexities of the bearings, was analyzed. Shahgoli et al. [10] analyzed the primary frequency of a symmetric rotating system without a disk, where the shaft includes stretching nonlinearity, and validated the results using the multiple scales method. Rui et al. [11] investigated the dynamic behavior of a two-degree-of-freedom rotating system with an outer ring defect at subharmonic frequencies.

Alishverichi et al. [12] studied the dynamic response of a 2DOF system excited by a non-ideal exciter, where the system vibrates near the first critical speed.

In some cases, instead of using a conventional disk, a disk reinforced with graphene nanoplatelets or two conventional disks bolted together are used. this approach significantly reduces the system's vibration amplitude at various points [13].

Numerous studies have been conducted on the stability and nonlinear vibration analysis of rotor systems with flexible/rigid blades [14]. Some studies develop a nonlinear time-dependent model of the blade-rotor-bearing system using Lagrange's equation [15], where wires are used to connect the blades to reduce the system's vibration amplitude at resonance frequencies [16]. Linear and nonlinear supports are also used to model bearings in rotor-blade-bearing systems, which affect the system's dynamic response [17].

In this paper, a rotor-disk-bearing system with two disks positioned equidistantly and with zero-degree phase difference is studied, where the shaft exhibits significant elastic deformation under bending, necessitating the inclusion of geometric nonlinearities in the shaft modeling. The shaft is supported by flexible bearings, modeled as an equivalent spring-damper system with linear and nonlinear stiffness elements. The equations of motion for the rotating system, which include a flexible shaft, rigid disk, and flexible bearing, are derived using the extended Hamilton's principle. The shaft is assumed to be an Euler-Bernoulli beam, thus ignoring shear deformation and rotary inertia. The resulting equations are solved analytically using the method of multiple scales and numerically, with the results compared. The findings demonstrate a strong agreement between the two methods.

2. Mathematical modeling

To derive the dynamic equations of motion, the kinetic and potential energy of the system components and work of non-conservative forces must first be calculated [1]. these extracted energies are then substituted into Hamilton's equation to obtain the partial differential equations.

$$\delta \int_0^t (T_{total} - U_{total} + W_{nc}) dt = 0 \tag{1}$$

Figure 1. schematic diagram of the system

After deriving the kinetic energies of the shaft, disks and unbalanced masses, as well as potential energies of the shaft and bearings, the equations of motion in the y and z directions are obtained using the extended Hamilton's principle.

$$\begin{aligned}&-M_{ud1}\Omega^2\sin[\Omega t]-M_{ud2}r_2\Omega^2\sin[\Omega t]+K_l w+2K_{nl}w^3+C\dot{w}+M_{d1}\ddot{w}\\&+M_{d2}\ddot{w}+A\rho\ddot{w}-AEv'w'v''-\frac{1}{2}AEv'^2w''-\frac{3}{2}AEw'^2w''+2I_A\rho\Omega\dot{v}''\\&+I_{12}\Omega\dot{v}''-I_{21}\ddot{w}''-I_{22}\ddot{w}''-I_A\rho\ddot{w}''+EI_Aw''''=0\end{aligned} \tag{2}$$

$$\begin{aligned}&-M_{ud1}r_1\Omega^2\cos[\Omega t]-M_{ud2}r_2\Omega^2\cos[\Omega t]+K_l v+2K_{nl}v^3+C\dot{v}+M_{d1}\ddot{v}\\&+M_{d2}\ddot{v}+A\rho\ddot{v}-\frac{3}{2}AEv'^2v''-\frac{1}{2}AEw'^2v''-AEv'w'w''-2I_A\rho\Omega\dot{w}''-I_{11}\Omega\dot{w}''\\&-I_{12}\Omega\dot{w}''-I_{21}\ddot{v}''-I_{22}\ddot{v}''-I_A\rho\ddot{v}''+EI_A\ddot{v}''''=0\end{aligned} \tag{3}$$

Equations (2) and (3) represent the equations of motion for the system. to solve these equations, they must first be discretized using the Galerkin method. then, the resulting ordinary differential equations are then solved using numerical and analytical methods, such as the multiple scales method, to analyze the dynamic and vibrational behavior of the system under different conditions.

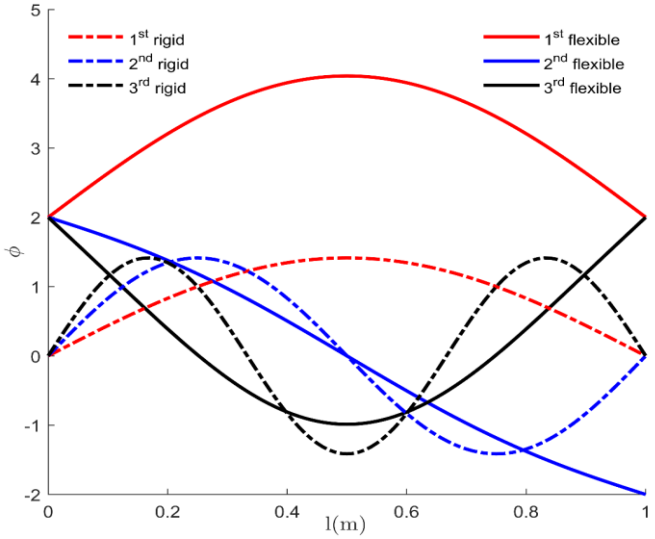

Figure 2. The mode shapes of the beam on rigid and flexible bearings

In Figure 2, the mode shapes of the beam for both elastic and rigid supports are illustrated. The beam on spring supports at both ends begins to oscillate from a value greater than zero in the first three modes, whereas for rigid supports, the starting and ending points of the beam are always zero[1]. To solve equations (2) and (3), which are the partial differential equations, we first need to transform them into ordinary differential equations using the first mode shape of the beam with two end spring supports. this is achieved using the Galerkin method. here, we will only use the first mode of the beam for discretizing the equations with the Galerkin method, as the first critical speed is crucial in designing and analyzing rotating systems. to accomplish this, $v = V(t)\varphi(x)$ and $w = W(t)\varphi(x)$ were substituted into the previous equations and then discretize them using the orthogonality property of the mode shapes. thus, the ordinary differential equations are obtained as below:

$$\ddot{w} + C\dot{w} + k_1\Omega\dot{v} + k_2 w - \mu v^2 w - k_4 w^3 = \Lambda_1 \sin(\Omega t) + \Lambda_2 \sin(\Omega t) \tag{4}$$

$$\ddot{v} + C\dot{v} - k_1\Omega\dot{w} + k_2 v - \mu w^2 v - k_4 v^3 = \Lambda_1 \cos(\Omega t) + \Lambda_2 \cos(\Omega t) \tag{5}$$

Equations (4) and (5) represent the system's equations of motion in the *y* and *z* directions, which were obtained after applying the Galerkin method and are now expressed solely in the time domain. The constants used in the above equations are obtained through the following relationships:

$$M = M_{d1}\varphi^2(x)\big|_{x=l_{d1}} + M_{d2}\varphi^2(x)\big|_{x=l_{d2}} - I_{21}\varphi(x)\frac{\partial^2}{\partial x^2}\varphi(x)\big|_{x=l_{d1}} - I_{22}\varphi(x)\frac{\partial^2}{\partial x^2}\varphi(x)\big|_{x=l_{d2}}$$
$$+\rho A\int_0^l \varphi(x)\frac{\partial^2}{\partial x^2}\varphi(x)dx - \rho I_A\int_0^l \varphi(x)\frac{\partial^2}{\partial x^2}\varphi(x)dx$$

$$k_1 = \frac{1}{M}(2\rho I_A\int_0^l \varphi(x)\frac{\partial^2}{\partial x^2}\varphi(x)dx + I_{11}\varphi(x)\frac{\partial^2}{\partial x^2}\varphi(x)dx\big|_{x=l_{d1}} + I_{12}\varphi(x)\frac{\partial^2}{\partial x^2}\varphi(x)dx\big|_{x=l_{d2}}$$

$$k_2 = \frac{EI_A}{M}\int_0^l \varphi(x)\frac{\partial^4}{\partial x^4}\varphi(x)dx + \frac{K_l\varphi^2(x)\big|_{x=0} + K_l\varphi^2(x)\big|_{x=l}}{M}$$

$$\mu = \frac{3}{2M}(EA\int_0^l \varphi(x)\frac{\partial^2}{\partial x^2}\varphi(x)\{\frac{\partial}{\partial x}\varphi(x)\}dx)$$

$$k_4 = \frac{3}{2M}(EA\int_0^l \varphi(x)\frac{\partial^2}{\partial x^2}\varphi(x)\{\frac{\partial}{\partial x}\varphi(x)\}dx) - \frac{2K_{nl}}{M}(\varphi^4(x)\big|_{x=0} + \varphi^4(x)\big|_{x=l})$$

$$\Lambda_1 = \frac{m_{u1}\Omega^2 r_1\varphi(l_{d1})}{M}\ ,\ \Lambda_2 = \frac{m_{u2}\Omega^2 r_2\varphi(l_{d2})}{M}\ ,\ C = \frac{c}{M} \tag{6}$$

3. Perturbation technique: Method of multiple scales

After determining the constants, the method of multiple scales is employed to solve equations (4) and (5) In this approach, the responses of the system in both vibrational directions are considered as functions of time and epsilon, where epsilon is a very small perturbation parameter [18].

$$V(t,\varepsilon) \approx V_0(T_0,T_1) + \varepsilon V_1(T_0,T_1) \tag{7}$$

$$W(t,\varepsilon) \approx W_0(T_0,T_1) + \varepsilon W_1(T_0,T_1) \tag{8}$$

As mentioned, to solve the differential equations (4) and (5), V and W are considered as polynomials in terms of T_0 and T_1, and substituted into the differential equations. Since the equations are of second order, and the first and second derivatives of V and W are required, the following relationships are used for these derivatives[18]:

$$T_n = \varepsilon^n t, n = 0,1,2,\ldots \ , \ T_0 = t \ , \ T_1 = \varepsilon t \ , \ D_n = \frac{\partial}{\partial \tau_n} \tag{9}$$

$$\frac{d}{dt} = \frac{dT_0}{dt}\frac{\partial}{\partial T_0} + \frac{dT_1}{dt}\frac{\partial}{\partial T_1}\ldots \ , \ \frac{d}{dt} = D_0 + \varepsilon D_1 + \ldots \tag{10}$$

$$\frac{d^2}{dt^2} = {D_0}^2 + 2\varepsilon D_0 D_1 + \varepsilon^2({D_1}^2 + 2D_0 D_2) \tag{11}$$

In the method of multiple scales, the system must be weakly nonlinear, meaning this method is applicable for weak nonlinearities. Since the imbalance is small compared to the diameter of the shaft, the nonlinear coefficients are small, and the method of multiple scales can be used. for this purpose, the values of C, μ, k_4, Λ_1, and Λ_2 are replaced with ϵC, $\epsilon\mu$, ϵk_4, $\epsilon\Lambda_1$, and $\epsilon\Lambda_2$, respectively[1]. by considering the above expressions and and substituting expressions (7) to (11) into the differential equations (4) and (5), terms with coefficients ϵ^0 and ϵ^1 are obtained.

System of order zero equations (ϵ^0):

$${D_0}^2 W_0 - \Omega_2 k_1 D_0 V_0 + k_2 W_0 = 0 \tag{12}$$

$${D_0}^2 V_0 - \Omega_2 k_1 D_0 W_0 + k_2 V_0 = 0 \tag{13}$$

System of order one equations (ϵ^1):

$$\begin{aligned} &{D_0}^2 W_1 + k_2 W_1 - \Omega k_1 D_0 V_1 = \Omega k_1 D_0 V_0 - 2D_1 W_0 - \mu W_0 {V_0}^2 - v_4 {W_0}^3 - cD_0 W_0 \\ &+\Lambda_1 \sin(\Omega t) + \Lambda_2 \sin(\Omega t) \end{aligned} \tag{14}$$

$$\begin{aligned} &{D_0}^2 V_1 + k_2 V_1 - \Omega k_1 D_0 W_1 = \Omega k_1 D_0 W_0 - 2D_1 V_0 - \mu V_0 {W_0}^2 - v_4 {V_0}^3 - cD_0 V_0 \\ &+\Lambda_1 \cos(\Omega t) + \Lambda_2 \cos(\Omega t) \end{aligned} \tag{15}$$

The homogeneous solution of equations (12) and (13) are provided in [1].By substituting the homogeneous solutions into equations (12) and (13) and then solving the quadratic equations for β_f and β_b, the linear natural frequencies of the forward and backward modes are obtained:

$$\beta_{f,b} = \frac{1}{2}(\Omega k_1 \pm \sqrt{\Omega^2 {k_1}^2 + 4k_2}) \tag{16}$$

To analyze the stability of the system in the steady-state condition, we set the angular velocity of the excitation of the unbalanced mass near the system's natural precession frequency, $\Omega = \beta_f + \varepsilon\sigma$. since, in primary resonance, only forward frequency is excited [8]; now, by substituting the homogeneous solutions of equations (12) and (13) in to the right-hand side of equations (14) and (15), we identify the terms that have the coefficient $e^{\beta_f T_0 i}$. then, by setting the coefficients of $e^{\beta_f T_0 i}$ and $e^{\beta_b T_0 i}$ to zero, and assuming $A_n = \frac{1}{2} a_n e^{i\Phi_n}$ and $\Upsilon = -\Phi_1 + \sigma T_1$, and separating the real and imaginary parts of the equations and may set up, $\dot{a}_1 = 0$, $\dot{a}_2 = 0$, $\dot{\Phi}_1 = 0$ and $\dot{\Phi}_2 = 0$ to obtain the steady-state response, an implicit equation in terms of the tuning frequency and amplitude obtained:

$$\frac{4}{(\Lambda_1+\Lambda_2)^2}\left(\frac{3}{8}k_4 a_1(T_1)^3+\frac{1}{8}\mu a_1(T_1)^3+\beta_f a_1(T_1)\sigma(T_1)\right.$$
$$\left.-\frac{1}{2}k_1\Omega a_1(T_1)\sigma(T_1)\right)+\frac{(C\beta_f a_1(T_1))^2}{(\Lambda_1+\Lambda_2)^2}=1 \quad (17)$$

4. Results and discussion

After solving the implicit equation obtained from the method of multiple scales and numerically solving equations (4) and (5) using the Runge-Kutta method. Figure 3(right) illustrates the Campbell diagram of the rotating system. In rotating systems, due to the presence of gyroscopic forces, the natural frequency of the system is not constant and varies with the rotational speed. This diagram is plotted using equation (16), showing the forward and backward frequencies as a function of the system's rotational speed. The greater the linear stiffness, the higher the value of β_f, meaning the system will resonate at higher frequencies. Figure 3(left) shows that due to the presence of nonlinear stiffness in the bearing, the frequency response of the beam with both ends supported by springs shifts to the right, and the oscillation amplitude decreases. according to this chart, nonlinear stiffness in the bearing has a significant effect on the frequency response curve. the greater the nonlinear stiffness, the more the curve bends to the right, indicating the hardening effect of the system [1]. the nonlinear stiffness does not affect the natural frequency and critical speed of the system by solving equation (17), the system's frequency response is obtained, and by using the Jacobian matrix and the sign of the determinant's eigenvalues, the stable and unstable points can be identified [19]. in some areas, this diagram has three solutions: one trivial solution, one non-trivial unstable solution, and one larger stable solution. all the physical and geometric properties of the system are listed in Table 1.

Table 1. Parameters of the system

Parameters	Values	Parameters	Values
Shaft length (l)	1(m)	Modulus of elasticity (E)	200(GP_a)
Shaft radius (R)	0.02(m)	Viscous damping (c)	10(Ns/m)
Disk radius (R_d)	0.07(m)	Linear bearing stiffness (k_l)	9×10^5(N/m)
Disk thickness (h)	0.015(m)	Nonlinear bearing stiffness (k_{nl})	2×10^9(N/m)
Unbalance mass (M_{ud})	0.015(kg)	Density (ρ)	7800(kg/m^3)

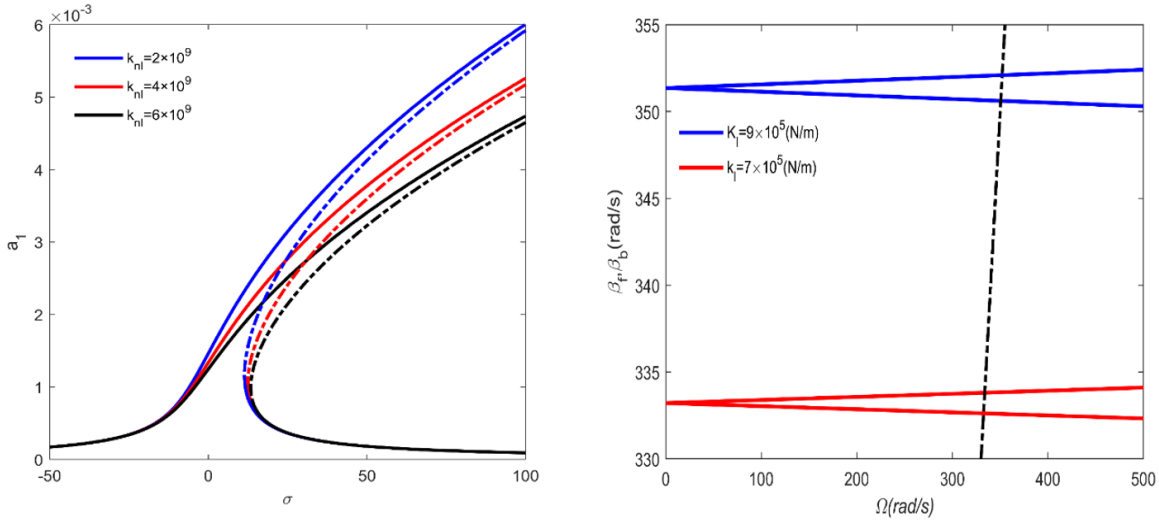

Figure 3. Frequency response curve for different values of bearing nonlinear stiffness(left) and campbell diagram(right)

Given that the shaft is modeled as a beam with both ends supported by springs, and the mode shape of this beam has been used for discretizing the equations via the Galerkin method, all the results are based on this mode shape. however, in Figure 4, the mode shape of a simply supported beam $\sin(n\pi x/l)$ is used, and the frequency response is compared with the model of the beam with both ends supported by springs. at some frequencies, the method of multiple scales has been validated against the numerical method, which also applies to the simply supported beam mode shape. Figure 5 shows the frequency response of the system, validated with four points using numerical methods. Points A_1, A_2, and A_4 are obtained with the initial condition $V(0)=6\times10^{-6}$, while point A_3 is obtained with the initial condition $V(0)=6\times10^{-2}$. The presence of geometric nonlinearity in the shaft modeling leads to a jump phenomenon in the frequency response curve. this phenomenon may occur at certain points known as bifurcation points. for instance, at point A_3 where the system oscillates at a specific tuning frequency, a slight increase in rotational frequency does not increase the amplitude as predicted by the curve; instead, the system's oscillation amplitude suddenly drops to a lower stable value (A_4).

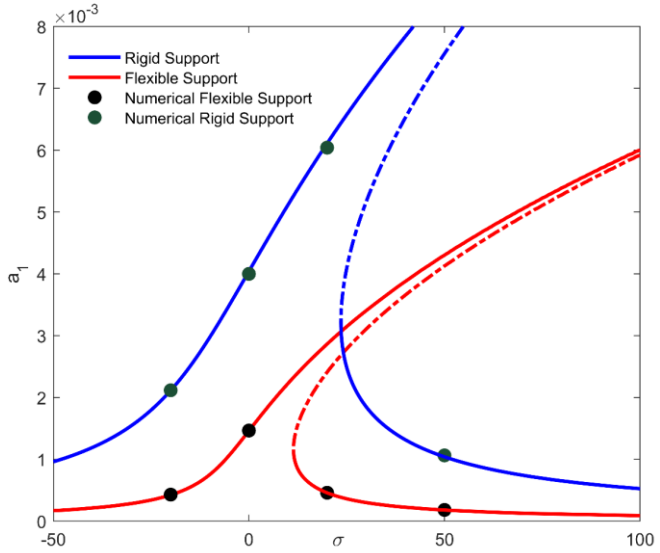

Figure 4. frequency response curves for flexible and rigid bearings

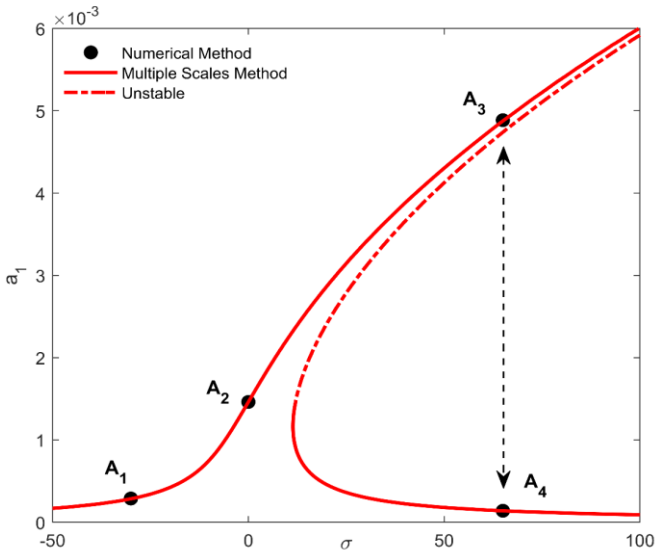

Figure 5. frequency response curve with different initial conditions

5. Conclusion

In this study, a nonlinear dynamic analysis of a rotor-disk-bearing system was conducted to investigate the impact of bearing flexibility and stiffness nonlinearity. The shaft was modeled as an Euler-Bernoulli beam supported by two springs representing the bearings. Analytical and numerical solution techniques were employed to fully characterize the system's dynamic behavior. The critical speed were found to differ depending on whether the shaft was modeled as simply supported or a beam on springs. Introducing bearing stiffness into the model lowered the system frequencies compared to a rigidly supported beam. Furthermore, increasing the nonlinear bearing stiffness shifted the frequency response curves to higher frequencies. Multiple scales analysis provided analytical solutions that closely matched numerical solutions obtained via Runge-Kutta integration, validating the modeling approach. In unstable regions, the system response was strongly dependent on initial conditions, with larger amplitudes producing upper branch oscillations and smaller amplitudes yielding lower branch motions. Overall, this work demonstrated that realistically modeling the shaft support through flexible bearings, rather than rigid supports, is crucial for accurate dynamical predictions. Incorporating bearing nonlinearity was also shown to influence the system characteristics. The findings enhance understanding of rotor-bearing system dynamics, which can aid in design and condition monitoring of rotating machinery.

REFERENCES

1. H. P. Phadatare and B. Pratiher, “Dynamic stability and bifurcation phenomena of an axially loaded flexible shaft-disk system supported by flexible bearing,” Proc. Inst. Mech. Eng. Part C J. Mech. Eng
2. M. Moradi Tiaki, S. A. A. Hosseini, and H. Shaban Ali Nezhad, “Nonlinear free vibrations analysis of overhung rotors under the influence of gravity,” Proc. Inst. Mech. Eng. Part C J. Mech. Eng
3. M. S. Sadooghi, S. E. Khadem, and S. Bab, “Dynamic behavior investigation of a rotating system by two methods of nonlinear modeling and finite element,” vol. 16, no. 8, pp. 303–314, 2016.
4. P. H. Jain and S. P. Bhosle, “Mathematical modeling, simulation and analysis of non-linear vibrations of a ball bearing due to radial clearance and number of balls,” Mater.
5. Liang, M., Yan, T., Hu, J., & Chen, Z. (2020). Effect of rolling bearing parameters on the nonlinear dynamics of offset rotor. *Proceedings of the Institution of Mechanical Engineers*
6. M. K. Al-Solihat and K. Behdinan, “Force transmissibility and frequency response of a flexible shaft–disk rotor supported by a nonlinear suspension system,” *Int. J. Non. Linear. Mech.*
7. H. Zhang, K. Lu, W. Zhang, and C. Fu, “Investigation on dynamic behaviors of rotor system with looseness and nonlinear supporting,” *Mech. Syst. Signal Process.*, vol. 166, no. September 2021
8. S. E. Khadem, M. Shahgholi, and S. A. A. Hosseini, “Primary resonances of a nonlinear in-extensional rotating shaft,” *Mech. Mach. Theory*, vol. 45, no. 8, pp. 1067–1081, 2010
9. G. Zuo, L. Hou, R. Lin, S. Ren, , “Combination resonance and primary resonance characteristics of a dual-rotor system under the condition of the synchronous impact of the inter-shaft bearing,”
10. M. Shahgholi and S. E. Khadem, “Primary and parametric resonances of asymmetrical rotating shafts with stretching nonlinearity,” Mech. Mach. Theory, vol. 51, pp. 131–144, 2012,
11. R. Yang, Y. L. Jin, L. Hou, and Y. S. Chen, “Super-harmonic resonance characteristic of a rigid-rotor ball bearing system caused by a single local defect in outer raceway,” Sci. China Technol.
12. G. F. Alışverişçi, H. Bayıroğlu, and G. Ünal, “Nonlinear response of vibrational conveyers with non-ideal vibration exciter: Primary resonance,” Nonlinear Dyn.
13. T. Y. Zhao, Y. S. Cui, Y. Q. Wang, and H. G. Pan, “Vibration characteristics of graphene nanoplatelet reinforced disk-shaft rotor with eccentric mass,” *Mech. Adv. Mater. Struct.*,
14. S. Bab, S. E. Khadem, A. Abbasi, and M. Shahgholi, “Dynamic stability and nonlinear vibration analysis of a rotor system with flexible/rigid blades,” Mech. Mach. Theory
15. L. Wang, D. Q. Cao, and W. Huang, “Nonlinear coupled dynamics of flexible blade-rotor-bearing systems,” Tribol. Int., vol. 43, no. 4, pp. 759–778, 2010, doi: 10.1016/j.triboint.2009.10.016.
16. H. She, C. Li, Q. Tang, and B. Wen, “Effects of blade’s interconnection on the modal characteristics of a shaft-disk-blade system,” Mech. Syst. Signal Process.

17. B. Li, H. Ma, X. Yu, J. Zeng, X. Guo, and B. Wen, “Nonlinear vibration and dynamic stability analysis of rotor-blade system with nonlinear supports,” Arch. Appl. Mech., vol
18. A. L. I. H. Nayfeh and U. Rofesaor, “OSCILLATIONS,” 1995
19. T. Y. Yukio Ishida, Related Titles Principles of Turbomachinery Critical Component Wear in Heavy Duty Engines Machinery Vibration and Rotordynamics Handbook of Noise and Vibration Mechanical Vibrations